

Modeling the Mass Distribution in Spiral Galaxies

Adrick H. Broeils

Stockholm Observatory, S-133 36 Saltsjöbaden, Sweden

Stéphane Courteau

KPNO/NOAO, P.O. Box 26732, Tucson, Arizona 85726, USA

Abstract. We use deep r -band photometry and $\text{H}\alpha$ rotation curves for a sample of 290 late-type spirals to model their mass distribution within the optical radius. We examine luminosity profile decompositions into bulge and disk carefully and confirm that bulge light is best modeled by a seeing-convolved exponential profile. The optical rotation curves are well-reproduced with a combination of bulge and “maximum” disk components only. No dark halo is needed. The disk mass-to-light ratios (M/L ’s) correlate with the “size” of galaxies, as measured by mass, luminosity, or disk scale length. Correcting for this scale effect yields a narrow distribution of intrinsic M/L ’s for this galaxy population. By combining these models with HI data for other samples, we confirm that the luminous mass fraction increases with galaxy “size”.

1. Introduction

In order to improve our knowledge of the distribution and amount of luminous and dark matter (DM) in spiral galaxies, one has to construct mass models to reproduce the observed rotation curves (RCs) in detail (e.g. see review by van Albada in this volume). This can only be done by using extended HI RCs which sample the matter distribution far beyond the stellar disk. A troubling feature of these models is, however, the unknown scaling of the light distribution to a mass distribution in the form of a free M/L ratio. This uncertainty limits us to determining only the relative contributions of disk, bulge and dark components to the gravitational potential by making certain assumptions for the M/L ratios of the luminous components. The most widely used alternative is to maximize the contributions of these components to the observed RC (“maximum disk hypothesis”). One of the arguments for using a maximum disk is that optical RCs are very well reproduced by a combination of luminous components only. New data for the Milky Way also seem to be in agreement with a maximum disk solution with an M/L typical for Sb–Sc galaxies (Sackett 1996). In this paper we investigate the distribution of disk M/L ratios obtained from optical RCs (without the use of a DM component), and try to determine the width of the intrinsic (i.e. “scale”-free) M/L distribution.

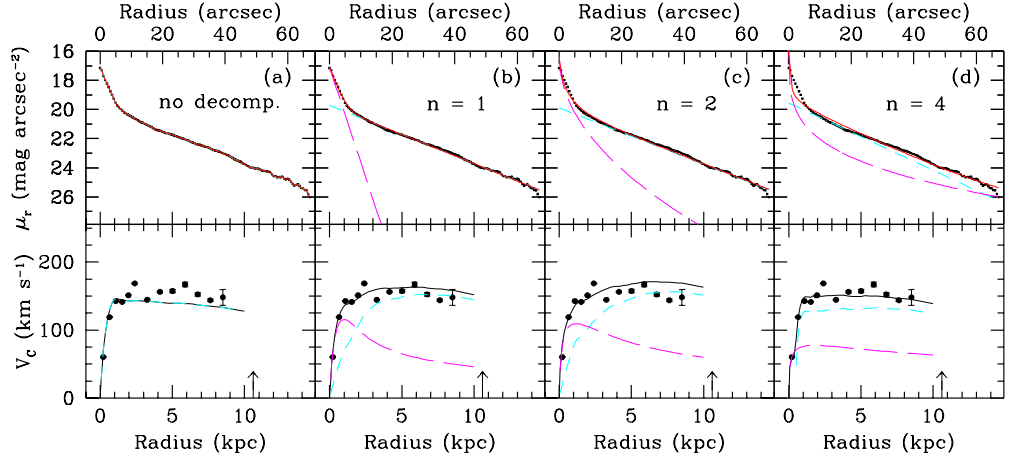


Figure 1. Examples of bulge-disk decompositions (top panels) using Sérsic bulge laws with $n = 1, 2$, and 4 (long-dash) + exponential disk (short dash) and the corresponding mass decompositions (bottom panels) for UGC 9097 ($b - d$). The SB fit is generally poorer with greater n , even for galaxies with substantial bulges like this one. A model without B/D decomposition fails to reproduce to observed RC (a). The arrow shows the location of R_{24} .

2. Sample

We have used data from the large collection of deep r -band photometry and $\text{H}\alpha$ RCs of Sb and Sc galaxies by Courteau (1992, 1996a, 1997). The sample was originally selected for Tully-Fisher mapping of peculiar velocities in the Northern Hemisphere. It includes Sb–Sc galaxies from the UGC catalog with inclinations between $50^\circ < i < 80^\circ$, which makes this sample well suited for mass modeling studies. From the original published collection of 350 spirals, we selected 290 galaxies with data of suitable quality to fit mass models to the optical RCs. The available data base is briefly described below; more detailed information about the photometric and spectroscopic observations can be found in (Courteau 1996a) and (Courteau 1997).

The one-dimensional r -band surface brightness (SB) profiles were obtained with 1m-class telescopes at Lick, Palomar, and Kitt Peak observatories. Repeat observations taken for almost half of the total observed sample and comparisons with the r -band photometry of Kent (1984, 1986) and Willick (1991) both indicate that the photometry is reliable down to 26 r -mag arcsec^{-2} and that the total r -band magnitudes are accurate to $\pm 0^m.08$.

Spectroscopic observations were made with the UV Schmidt spectrograph at the Lick 3m telescope. Exposure times were typically 1800 s which yields a sampling of the $\text{H}\alpha$ RCs out to about one optical radius (R_{24} , defined at the 24 r -mag arcsec^{-2} isophotal level). For the purpose of mass modeling, the observed RCs were folded and averaged about their centers. After inspection of each rotation curve, a transition radius was determined just beyond the central

solid-body rise. The averaged, folded RCs were then re-sampled at intervals of $2''$ (average seeing of all observations) within the transition radius; beyond that, the bins were doubled in size to improve the S/N in the fainter regions of the disk. Line-of-sight velocities were deprojected using disk inclinations determined from the photometry. A correction for redshift broadening was also applied. Seventy-six galaxies were observed more than once and their folded RCs were combined by taking the weighted average velocity within each bin.

We also retrieved IRAS $60\mu\text{m}$ fluxes f_{60} for 189 sample galaxies from the IRAS Faint Source Catalog through NED (NASA/IPAC Extragalactic Database). These provide an estimate of the star formation rate and will be used in our discussion in § 4.1. The conversion from observed ($''$) to physical (kpc) units uses heliocentric redshifts and $H_0 = 70\text{ km s}^{-1}\text{ Mpc}$.

3. Luminosity Decompositions

3.1. B/D decomposition technique

It has become clear that one must derive bulge and disk parameters simultaneously in order to obtain reliable decompositions (Kormendy 1977). The method we adopt is to fit model functions to the bulge and disk profiles (in the magnitude regime) using a non-linear χ^2 minimalization routine. The sum of disk and bulge model functions were convolved with a Gaussian-shaped PSF (with the appropriate seeing FWHM) before it was fitted to the observed profile.

A fundamental aspect of the decompositions is the choice of fitting functions. While the exponential nature of disk profiles has clearly been established (Freeman 1970), the true shape of bulge profiles in late-type spirals appears to have eluded the majority of workers in the field. Data now suggest that late-type bulges would be more accurately represented by an exponential profile instead of the long-assumed de Vaucouleurs law. Historical developments are discussed in Courteau et al. (1996) and Courteau (1996b).

To test for the shape of bulge luminosity profiles, we adopt the formulation of Sérsic (1968) who showed that exponential and de Vaucouleurs profiles are special cases of the general power law:

$$\Sigma(r) = \Sigma_0 \exp \left[- (r/r_0)^{1/n} \right], \quad (1)$$

where Σ_0 is the central brightness, r_0 is a scaling radius, and the exponent $1/n$ is a free variable. $n = 1$ corresponds to an exponential profile and the $n = 4$ case is equivalent to a de Vaucouleurs law.

3.2. Double exponential decompositions

Because many SB profiles often show unevenness (bumps and wiggles), it is not always possible to determine the best value of n reliably for most galaxies in our sample. These irregularities are often explained by the presence of regions of enhanced star formation, spiral arms, bars or other asymmetries in the 2-D light distribution. A significant fraction of SB profiles are of Freeman type II, defined by Freeman (1970) as a profile with a dip (near the bulge/disk transition) with respect to the exponential fit from the outer disk. Indeed, our sample is

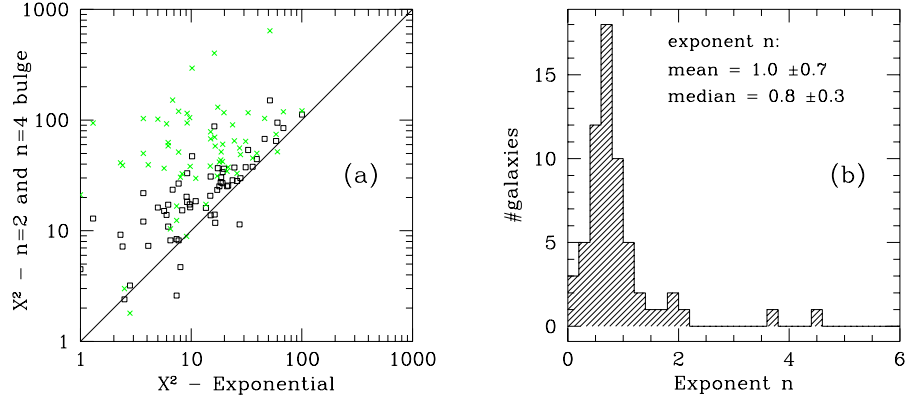


Figure 2. (a) Comparison of χ^2 values for models with $n = 2$ (squares) and 4 (crosses) with exponential bulge models for the SB profiles of the “clean” sub-sample. (b) Histogram of the exponent n with the lowest χ^2 in the fit.

about equally divided between Freeman types I and II. In order to establish the best fitting bulge function for the late-type systems, we first selected galaxies with smooth Freeman type I SB profiles and with a noticeable central (bulge-like) component. A total of 63 galaxies were selected for a combination of 90 independently-determined SB profiles.

Even with this “cleaner” sub-sample, solving for all five parameters (μ_d , r_d , μ_b , r_b , and n) simultaneously would be fraught with danger. Due to the paucity of data points at the center, the simultaneous solution of three bulge parameters is poorly constrained at best. Instead, we solve for a range of *fixed* values of n with the other four parameters unconstrained. An acceptable solution was usually reached within 10 or fewer iterations.

The upper panels of Fig. 1 show examples of bulge + disk decompositions with values of $n = 1, 2, 4$ for UGC 9097, a strong-bulged spiral by late-type standards. The quality of the match is usually best judged in the transition region between the bulge and inner disk. The failure of the $r^{1/4}$ profile is quite noticeable. Indeed, for nearly all the SB profiles, exponential bulges yield the lowest χ^2 values. This is demonstrated in Fig. 2a which shows the distribution of χ^2 ’s for $n = 2$ (squares) and 4 (crosses) against the one for exponential bulges.

We sampled values of n between 0.2 and 6 in steps of 0.2, and determined for each profile the “best” value of n corresponding to the lowest χ^2 . The distribution of “best” n values, shown in Fig. 2b, peaks at a value of $n = 0.8$, i.e. nearly exponential profiles. The ratio of bulge-to-disk exponential scale lengths (not shown here) is close to 0.1, as predicted by N-body simulations of secular evolution models (Courteau et al. 1996, Courteau 1996b). In agreement with other recent studies (see e.g. Courteau et al. 1996, and references therein), we conclude from this that the central regions of late-type spirals are best fit by exponential profiles, rather than the de Vaucouleurs law or an $n = 2$ bulge. For the remainder of this paper, SB profiles will only be modeled as a combination of two exponentials for the bulge and disk respectively.

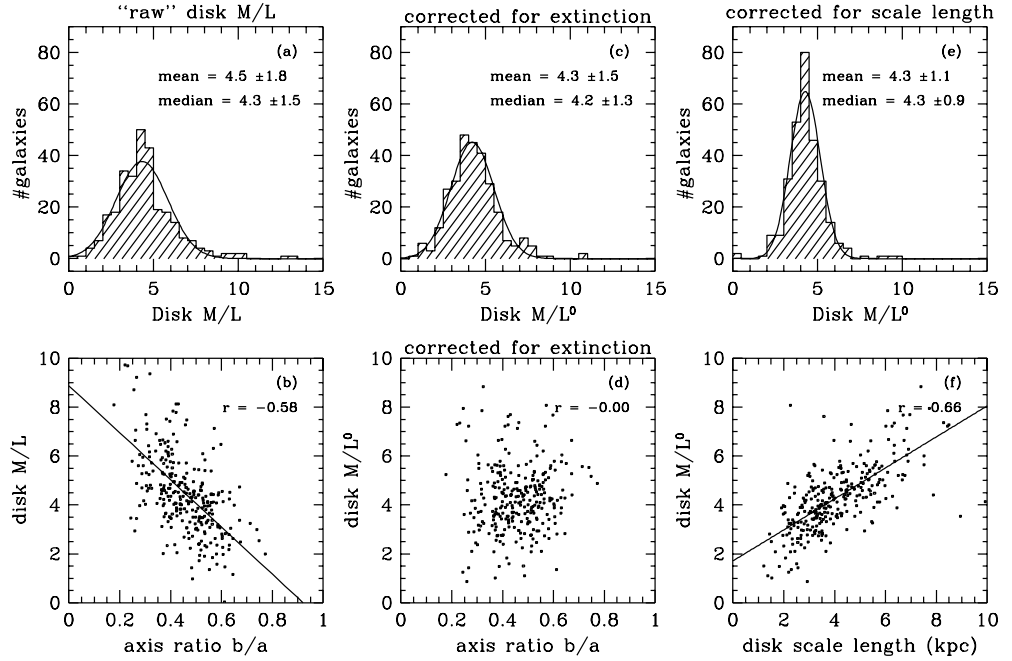


Figure 3. (a) Histogram of “raw” disk M/L , (b) dependence of M/L on axis ratio b/a , (c) histogram of “face-on” M/L , (d) M/L after b/a correction, (e) histogram of M/L^0 corrected for “size” using h , (f) dependence of M/L^0 on h .

4. Mass Decompositions

Modeling of the observed rotation curves follows the non-linear least-squares procedure outlined by Kent (1986) and Broeils (1992) (see also review by van Albada in this volume). The basic assumption is that the gravitational potential of a galaxy can be described as the sum of potentials of individual mass components, like stellar bulge and disk, gas disk, dark halo, etc. In all cases, the radial distribution of visible mass is assumed to be given by the mean radial distribution of light obtained from the B/D decompositions of the SB profiles. The bulge and disk M/L ’s are allowed to vary independently but remain constant (as a function of radius) within each component. The observed RCs are well fitted by the luminous components alone. These data provide little support for a dark component, and therefore its contribution has not been included in the mass models. This also means that the M/L ’s derived in this way are true “maximum” disk (and bulge) values, since inclusion of gas and dark matter will only lower these values.

The model disk and bulge rotation velocities are sampled at the same radii as the observed rotation curve, added in quadrature using the M/L ’s as free scaling parameters, and fitted to the observed rotation curve. All fits were visually inspected and occasionally the bulge contribution was adjusted manually

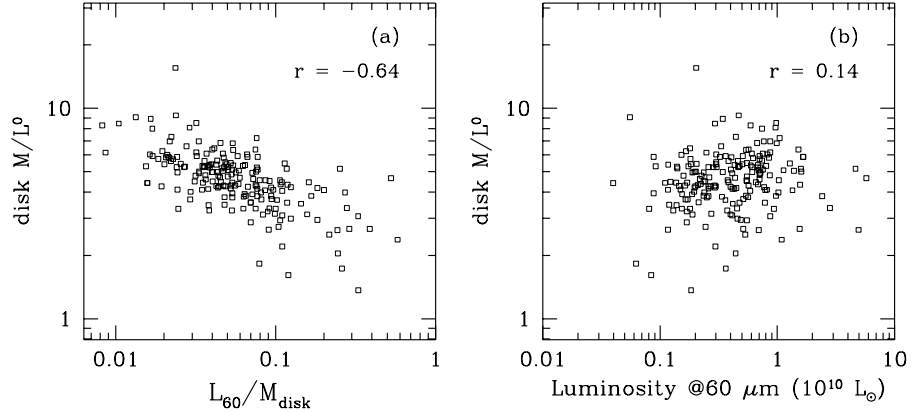


Figure 4. (a) Disk M/L versus L_{60}/M . L_{60}/M is proportional to the SFR per unit mass. (b) Disk M/L versus L_{60} . No apparent trend is visible. The correlation coefficients are shown in the upper right-hand corners.

(M/L_{bulge} set to maximum allowed value), especially in cases where the number of data points in the central region was insufficient to constrain the fits.

4.1. Results

We shall now examine the variation of M/L (from here onwards, M/L will refer to *disk* M/L) among galaxies and try to understand the processes causing this variation. Fig. 3a shows the distribution of the “raw” M/L from the mass decomposition of the rotation curves. The r -band luminosities used to estimate M/L were corrected for Galactic extinction only, but these (and consequently the M/L ’s) need to be corrected for internal extinction as well. Unfortunately, there is no trivial and accepted way to do this due to our very limited understanding of radiation transfer and sources of opacity in galaxies (e.g. see conf. proc. on this subject, Davies & Burstein 1995). The inclination dependence of M/L ’s was removed empirically by fitting the observed trend against ellipticities. Figure 3b shows the dependence of the “raw” M/L ’s on ellipticity; the line indicates the fit used to correct to “face-on” ratios.

Application of this correction reduces the width of the M/L distribution by 17% (see Fig. 3c,d). The corrected values still show a fairly broad distribution given the narrow range of galaxy types (Sb–Sc). One can appreciate that the mass in these M/L ’s is dominated by the old disk population, whereas a larger population of stars contributes to the r -band galaxian flux. Indeed, Rhee & van Albada (1996) recently argued that a large part of the M/L scatter is due to variations in star formation rates (SFRs) among galaxies. These authors used L_{60}/M as an indicator of the present SFR per unit mass (their M comes from a maximum-disk fit analogous to ours), to expose a clear correlation between $\log(M/L)$ and $\log(L_{60}/M)$ using the Rubin/Kent sample (Rubin et al. 1985; Kent 1986). Galaxies with a prominent young population have low M/L ’s which, they infer, would be due to enhanced star formation. This trend is also visible in our sample as shown in Fig. 4a. However the lack of correlation between M/L

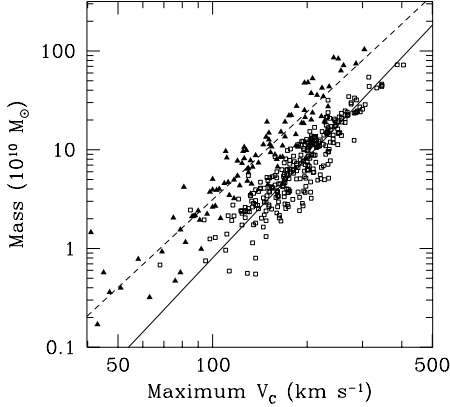


Figure 5. Mass versus maximum rotation velocity. The open symbols indicate luminous mass, filled triangles indicate total mass obtained from Broeils & Rhee (1997). The figure indicates that luminous mass fraction (solid line) increases with size.

and L_{60} (a more direct indicator of the SFR) shown in Fig. 4b suggests that the above effect is most likely due to a correlation between M/L and the mass of the stellar disk, contrary to the interpretation of Rhee & van Albada (1996).

It is not clear if the mass of the stellar disk itself is the fundamental physical parameter, but one could argue that the “size” of the galaxy is an important scaling parameter. The “size” of a galaxy could be measured by its (disk) mass, luminosity, linear size or disk scale length (h) since these parameters are all tightly coupled via the Tully-Fisher relation. The dependence of M/L ’s on the scaling parameter h is shown in Fig. 3f. Compact galaxies have low M/L ’s and big galaxies have large M/L ’s. If we take out this scaling effect using the fitted line in Fig. 3f, we obtain the histogram plotted in panel 3e. The spread in M/L can now be completely accounted for by a random error of about 15% in the distances to these galaxies. Similar projected distributions can be obtained by correcting the M/L ’s for disk mass and luminosity (Broeils & Courteau 1997).

Finally, we combine the results from our mass models with those from HI data on separate galaxies (Broeils & Rhee 1997) to show that the dark matter fraction in galaxies, expressed as the dark-to-luminous mass fraction $M_{\text{dark}}/M_{\text{lum}}$, also depends on a structural (“size”) parameter. The optical RCs themselves do not extend far enough to allow for the detection of DM. However, they provide a good estimate of the total luminous mass¹ and of the dependence of this mass on “size”. The open squares in Fig. 5 indicate the *luminous* mass of the 290 galaxies used in this study, and the full line is a linear fit to these data points. In lieu of scalelengths, the maximum rotation velocity (V_{max}) acts as the “size” parameter. The filled triangles represent *total* masses obtained from 1-D HI spectra of 103 galaxies (Broeils & Rhee 1997) (fitted with a dashed line). It is obvious that the luminous mass fraction (with respect to the total

¹So long as the mass model fits indicate that the amount of dark matter in regions sampled by the optical RCs is small.

mass) increases systematically with bigger galaxy size. Thus, for arbitrary large systems and if the maximum-disk hypothesis holds true, the amount of dark matter per galaxy becomes negligible. The increase of luminous mass fraction with galaxy size has been known for quite some time based on optical RCs alone (Persic & Salucci 1988, 1990) and HI RCs (Broeils 1992, and references therein); the presentation here shows the trend for much larger and completely independent samples. While the slope from the HI samples is fixed, that of our optical decompositions depends highly on the assumption of maximum-disk (as in the case of detailed mass models for extended RCs). A more important contribution of the dark matter to the inner disk would cause the trend to flatten.

5. Conclusions

We find that the luminosity distributions of bulges of Sb–Sc galaxies are best fitted by exponential profiles. Using such profiles, we find that the ratio of bulge-to-disk scale lengths is close to 0.1, as predicted by simulations of secular evolution. Disk M/L 's obtained from maximum-disk fits to optical RCs correlate well with galaxy “size”. Correcting for this “size” effect yields a narrow distribution of intrinsic M/L 's, which can be fully accounted for by 15% distance errors.

References

Broeils, A. H. 1992, Ph.D. thesis, Univ. of Groningen, the Netherlands
 Broeils, A. H., & Courteau, S. 1997, in preparation
 Broeils, A. H., & Rhee, M. H. 1997, A&A, in press
 Courteau, S. 1992, Ph.D. thesis, Univ. of California, Santa Cruz
 Courteau, S. 1996a, ApJS, 103, 363
 Courteau, S. 1996b, in New Extragalactic Perspectives in the New South Africa: Changing Perceptions of the Morphology, Dust Content and Dust-Gas Ratios in Galaxies, ed. D. Block, M. Greenberg (Dordrecht: Kluwer), 255
 Courteau, S. 1997, ApJS, submitted
 Courteau, S., de Jong, R. S., & Broeils, A. H. 1996, ApJ, 457, L73
 Davies, J. I., & Burstein, D. 1995, Opacity in Spiral Disks (Dordrecht: Kluwer)
 Freeman, K. C. 1970, ApJ, 160, 811
 Kent, S. M. 1984, ApJS, 56, 105
 Kent, S. M. 1986, AJ, 91, 1301
 Kormendy, J. 1977, ApJ, 217, 406
 Persic, M., & Salucci, P. 1988, MNRAS, 234, 131
 Persic, M., & Salucci, P. 1990, MNRAS, 245, 577
 Rhee, M. H., & van Albada, T. S. 1996, MNRAS, submitted
 Rubin, V. C., Burstein, D., Ford, J. W. K., & Thonnard, N. 1985, ApJ, 289, 81
 Sackett, P. D. 1996, ApJ, submitted
 Sérsic, J. L. 1968, Atlas de Galaxias Australes (Córdoba: Observ. Astronomica)
 Willick, J. A. 1991, Ph.D. thesis, Univ. of California, Berkeley